

See discussions, stats, and author profiles for this publication at: <https://www.researchgate.net/publication/233872613>

Kinetic Water Stability of an Isostructural Family of Zinc-Based Pillared Metal-Organic Frameworks

ARTICLE *in* LANGMUIR · DECEMBER 2012

Impact Factor: 4.46 · DOI: 10.1021/la304204k · Source: PubMed

CITATIONS

36

READS

126

5 AUTHORS, INCLUDING:



[Himanshu Jasuja](#)

Georgia Institute of Technology

16 PUBLICATIONS 477 CITATIONS

[SEE PROFILE](#)



[Nicholas Burtch](#)

Georgia Institute of Technology

8 PUBLICATIONS 135 CITATIONS

[SEE PROFILE](#)

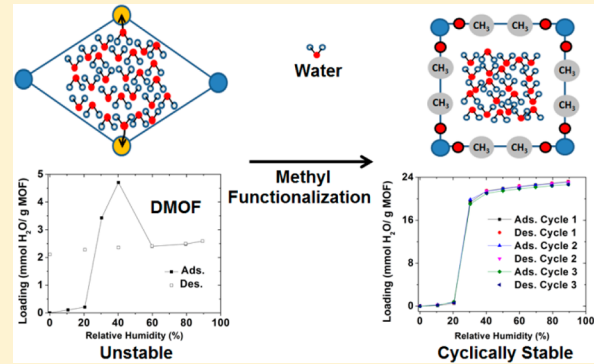
Kinetic Water Stability of an Isostructural Family of Zinc-Based Pillared Metal–Organic Frameworks

Himanshu Jasuja, Nicholas C. Burtch, You-gui Huang, Yang Cai, and Krista S. Walton*

School of Chemical and Biomolecular Engineering, Georgia Institute of Technology, 311 First Drive NW, Atlanta, Georgia 30332, United States

 Supporting Information

ABSTRACT: The rational design of metal–organic frameworks (MOFs) with structural stability in the presence of humid conditions is critical to the commercialization of this class of materials. However, the systematic water stability studies required to develop design criteria for the construction of water-stable MOFs are still scarce. In this work, we show that by varying the functional groups on the 1,4-benzenedicarboxylic acid (BDC) linker of DMOF $[Zn(BDC)(DABCO)]_{0.5}$, we can systematically tune the kinetic water stability of this isostructural, pillared family of MOFs. To illustrate this concept, we have performed water adsorption studies on four novel, methyl-functionalized DMOF variations along with a number of already reported functionalized analogues containing polar (fluorine) and nonpolar (methyl) functional groups on the BDC ligand. These results are distinctly different from previous reports where the apparent water stability is improved through the inclusion of functional groups such as $-CH_3$, $-C_2H_5$, and $-CF_3$ which only serve to prevent significant amounts of water from adsorbing into the pores. In this study, we present the first demonstration of tuning the inherent kinetic stability of MOF structures in the presence of large amounts of adsorbed water. Notably, we demonstrate that while the parent DMOF structure is unstable, the DMOF variation containing the tetramethyl BDC ligand remains fully stable after adsorbing large amounts of water vapor during cyclic water adsorption cycles. These trends cannot be rationalized in terms of hydrophobicity alone; experimental water isotherms show that MOFs containing the same number of methyl groups per unit cell will have different kinetic stabilities and that the precise placements of the methyl groups on the BDC ligand are therefore critically important in determining their stability in the presence of water. We present the water adsorption isotherms, PXRD (powder X-ray diffraction) patterns, and BET surface areas before and after water exposure to illustrate these trends. Furthermore, we shed light on the important distinction between kinetic and thermodynamic stability in MOFs. Molecular simulations are also used to provide insight into the structural characteristics governing these trends in kinetic water stability.



1. INTRODUCTION

Metal–organic frameworks (MOFs) are a relatively new class of nanoporous materials that have received significant attention due to their exceptionally high porosities and chemically tunable structures.^{1–6} As a result, MOFs have become ideal candidates for applications such as air purification, chemical sensing, hydrogen storage, catalysis, and CO_2 capture.^{7–13} MOFs are characterized by their metal-ion clusters and organic ligands. An increasing number of MOFs with highly desirable properties such as open-metal sites and amine-functionalized groups have been synthesized in the literature, giving them enormous potential for revolutionizing the adsorption field.⁹ Industrial adsorbents, e.g., those used in CO_2 capture applications, come in direct contact with moisture via the operating conditions and regeneration steps involved in the process. One key challenge in the commercialization of MOFs is a lack of fundamental understanding regarding the factors that influence their stability under humid conditions.

Despite the poor hydrothermal stability of many MOFs, reports on water adsorption and its subsequent impact on structural stability are scarce relative to other studies performed with gases such as CO_2 , CH_4 , N_2 , and H_2 . Carboxylate-based MOFs are especially prone to breakdown in the presence of humid conditions,^{14–18} a characteristic that has been attributed to the relatively weak metal–ligand bond formed between oxygen and the metal.¹⁹ However, notable exceptions to these trends are also present; for example, the chromium-based MIL-53 and MIL-101 structures are stable due to the inertness of the Cr metal,^{20,21} while UiO-66 and MIL-125 are stable due to the high nuclearity and coordination number of their secondary building units.^{21–23} Our group recently reported an experimental investigation into the loss of crystallinity and surface area caused by exposure to humid conditions in various

Received: October 23, 2012

Revised: December 4, 2012

Published: December 6, 2012



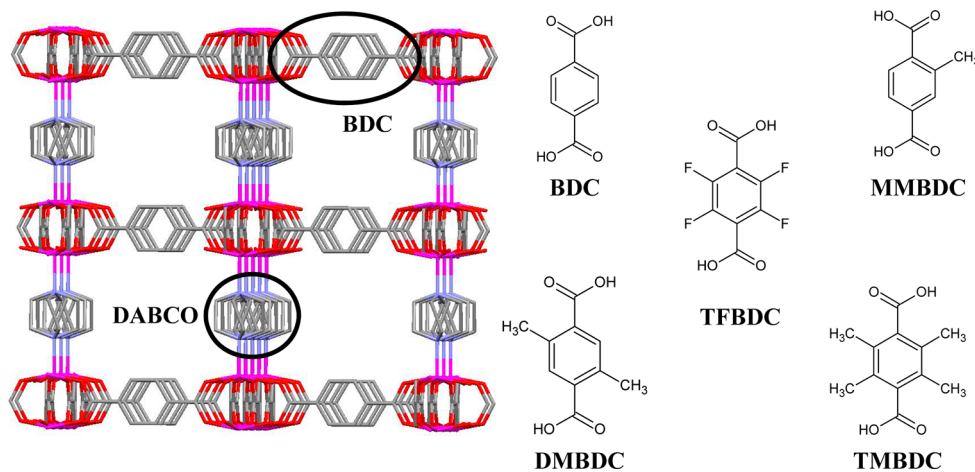


Figure 1. Left: the 3D structure of DMOF or $[Zn(BDC)(DABCO)_{0.5}]$. Hydrogen atoms are omitted for clarity. Color code: Zn, pink; O, red; C, gray; N, purple. Right: the functionalized BDC ligands used to synthesize the DMOF-X family.

prototypical MOF systems containing open-metal sites, amine-functional groups, carboxylate coordination, and nitrogen coordination.²⁴ Past studies have attempted to understand the poor hydrothermal stability of the well-studied IRMOF-1 experimentally²⁵ and computationally^{26–28} through the use of reactive force fields and first principles molecular dynamics simulations.

Long and co-workers were the first to showcase that, from a thermodynamic standpoint, MOF stability can be related to the basicity (pK_a) of the ligand.^{17,29} Because MOFs are derived from Lewis acid–base coordination complexes between metal ions and ligands, the pK_a of the isolated ligand can be used to predict the thermodynamic strength of the resulting metal–ligand bond. This work was further supported by Low et al.,¹⁹ who also found that the strength of the bond between metal oxide cluster and the bridging linker is important in defining the hydrothermal stability of various MOFs. Other studies have since been carried out under humid conditions to characterize the stability and water adsorption properties of MOFs such as MOF-177, Cu-BTC, ZIF-8, MIL-101(Cr), MIL-100(Fe), MIL-53 (Al, Cr, V), and UiO-66.^{14,19,20,30–35} From these studies it was concluded that, while 4-coordinated zinc–oxygen MOFs tend to be unstable in water,^{14,19,24} nitrogen-coordinated MOFs have better water stability due to the higher basicity (pK_a) of nitrogen-based ligands.^{24,31} By this same logic, MOFs with the highly basic pyrazolate ligand ($pK_a \sim 19.8$)²⁹ show outstanding thermodynamic stability upon exposure to humid conditions and boiling water,¹⁷ whereas the slightly lower basicity of imidazole-based MOFs ($pK_a \sim 18.6$)²⁹ such as ZIF-8 makes their structures stable after exposure to humid conditions³⁰ but not after prolonged exposure to liquid water.²⁵ In this case, the former series of pyrazolate-based MOFs have thermodynamic stability in the presence of liquid water, whereas the latter's stability is purely kinetic.²⁵ Recently, thermodynamic stability of two new MOFs MOOFOUR-1-Ni and CROFOUR-1-Ni was also confirmed since their as-synthesized samples retain crystallinity even when immersed in water for months, boiling water for 1 day, or 0.1 N NaOH for a week.³⁶

While acid–base effects are critical to determining the thermodynamic stability of MOFs in the presence of water, ligand functionalization can be seen as a promising approach for tuning the kinetic stability. Ma et al.¹⁵ compared the water stability of three isostructural, pillared MOFs built from zinc,

1,4-benzenedicarboxylic acid (BDC), and methyl-functionalized variations of the 4,4'-bipyridine (BPY) ligand. It was found that, while the addition of methyl groups to BPY enhanced the structural stability of the parent structure under humid conditions, the degree of improvement was sensitive to the specific placement of the methyl groups. In particular, the addition of methyl groups at the 2,2'-position on BPY resulted in a more water stable structure (SCUTC-18) than the one containing methyl groups at the 3,3'-position (SCUTC-19). It is interesting to note that while this point was not made in the original study, the pK_a values of the two functionalized ligands used in these isostructural MOFs are nearly the same ($pK_a = 5.58$ for SCUTC-18 vs $pK_a = 5.29$ for SCUTC-19).³⁷ As a result, one would not predict the thermodynamic stability of the two structures to largely differ; instead, differences in the kinetic stability of these structures are likely responsible for the observed differences in water stability. However, because no water vapor adsorption isotherms were reported, it is difficult to determine whether SCUTC-18 is more stable due to an inherent change in structural stability or simply from the exclusion of water from entering its pores due to the nonpolar methyl groups. Along these same lines, the incorporation of hydrophobic alkyl and trifluoromethyl functional groups have been shown to improve the apparent water stability of other MOF variations as well.^{16,38–42} However, similar to the study by Ma et al.,¹⁵ broader insight into the inherent stability of the MOF structures cannot be extracted.

To date, there are very few MOFs (e.g., UiO-66, MIL-100(Fe), MIL-101(Cr)) that remain stable after the adsorption of large amounts of water vapor.^{24,30,32,33} MOFs with open metal sites such as Cu-BTC or HKUST-1 and MOF-74 or CPO-27 are also quite hydrophilic; however, they degrade in humid air.²⁴ From a practical standpoint, preventing water from entering a porous material may be an acceptable short-term approach to improving its performance under humid conditions. However, during long exposure times, some amount of water will likely still adsorb into the pores of the framework, regardless of how hydrophobic the pores may be. Furthermore, from a fundamental standpoint, it is of much greater interest to understand how the inherent stability of a structure can be tuned so that it remains stable even after water has entered the pores. Such knowledge is critical to the development of design criteria for a broad range of next-

Table 1. Family of Isostructural Pillared MOFs in This Work

MOF	formula	tag	carboxylate ligand
[Zn(BDC)(DABCO) _{0.5}]		DMOF ^{24,43}	100% BDC
[Zn(BDC) _{0.5} (MMBDC) _{0.5} (DABCO) _{0.5}]		DMOF-MM1 ^a	50% BDC: 50% MMBDC
[Zn(MMBDC)(DABCO) _{0.5}]		DMOF-MM2 ^a	100% MMBDC
[Zn(BDC) _{0.5} (DMBDC) _{0.5} (DABCO) _{0.5}]		DMOF-DM1 ^a	50% BDC: 50% DMBDC
[Zn(DMBDC)(DABCO) _{0.5}]		DMOF-DM2 ^a	100% DMBDC
[Zn(BDC) _{0.5} (TMBDC) _{0.5} (DABCO) _{0.5}]		DMOF-TM1 ⁴³	50% BDC: 50% TMBDC
[Zn(TMBDC)(DABCO) _{0.5}]		DMOF-TM2 ⁴³	100% TMBDC
[Zn(TFBDC)(DABCO) _{0.5}]		DMOF-TF ⁴³	100% TFBDC

^aNew MOFs synthesized in this work.

generation, water-stable MOFs that are not necessarily hydrophobic in character.

Because there are so many interdependent factors which govern MOF stability under humid conditions (metal type and coordination state, framework dimensionality, interpenetration, etc.), it is desirable to keep as many of these variables constant as possible. As such, water adsorption and characterization studies on isostructural MOF series are critical to isolating the specific factors that govern structural stability. DMOF (Figure 1) is a mixed-ligand MOF that contains zinc clusters connected in the 2D plane by 1,4-benzenedicarboxylic acid (BDC) and the pillar linker 1,4-diazabicyclo[2.2.2]octane (DABCO) connecting the third dimension.⁴³ Because of the partial stability of the parent structure under humid conditions (until ~30% relative humidity),³¹ it provides the ideal system to systematically tune properties and study their resulting impact on water stability. In our previous work⁴⁴ we performed a water adsorption study on a series of structures in the DMOF family. The goal was to showcase that it is possible to adjust the water stability of a pillared MOF in both the positive and negative directions by proper functionalization of the BDC ligand. In this work, we have extended this concept by synthesizing four novel isostructural MOFs with methyl functional groups at different positions on the BDC linker. We have also performed water adsorption studies on these newly synthesized DMOF variations as well as a number of already reported functionalized analogues containing polar (fluorine) and nonpolar (methyl) functional groups on the BDC ligand (Table 1). Furthermore, we also calculated the pK_a values for the functionalized ligands to investigate whether the difference in structural stability among members of this isostructural, pillared family under humid conditions is thermodynamic or kinetic in nature. Through an analysis of molecular simulations, experimental water adsorption isotherms, PXRD patterns, and N_2 adsorption at 77 K before and after water exposure, we are able to obtain important insight into the impact of water adsorption on the observed trends in kinetic water stability of these structures.

2. EXPERIMENTAL AND SIMULATION DETAILS

2.1. Synthesis. All the required chemicals were used as procured (without any purification) from commercial suppliers: Sigma-Aldrich, *N,N'*-dimethylformamide (DMF), 2,3,5,6-tetrafluoro-1,4-benzenedicarboxylic acid (TFBDC); Combi-Blocks, 2-monomethyl 1,4-benzenedicarboxylic acid (MMBDC); TCI America, 2,5-dimethyl-1,4-benzenedicarboxylic acid (DMBDC); Chem Service Inc., 2,3,5,6-tetramethyl-1,4-benzenedicarboxylic acid (TMBDC); Acros, 1,4-diazabicyclo[2.2.2]octane (DABCO), 1,4-benzenedicarboxylic acid (BDC), methanol (MeOH).

By varying the functional group(s) added on the BDC linkers (Figure 1), we obtained an isostructural pillared MOF family, DMOF-X, as summarized in Table 1. DMOF-MM1, MM2, DM1, and DM2 are novel MOFs, whereas as DMOF-TM1, TM2, and TF are synthesized as reported in the literature.⁴⁵ DMOF-MM1, DM1, and TM1 were synthesized using equal amounts of BDC and the respective mono-, di-, and tetramethyl-functionalized BDC to obtain a material where only half of the BDC ligands are functionalized with methyl groups. However, DMOF-MM2, DM2, TM2, and TF were synthesized using only the indicated functionalized ligand. Detailed synthesis procedures are provided in the Supporting Information.

2.2. Characterization. **2.2.1. Single Crystal XRD (X-ray Diffraction).** Single crystal X-ray data of DMOF-DM1 and DMOF-DM2 were collected on a Bruker APEX II CCD sealed tube diffractometer by using Mo $K\alpha$ ($\lambda = 0.71073 \text{ \AA}$) radiation with a graphite monochromator. Crystals of the MOFs were mounted on nylon CryoLoops with Paratone-N. The structure was solved by direct methods and refined by full-matrix least-squared techniques using the SHELXTL-97 software suite. Crystallographic details are listed in Supporting Information (Table S2 and Figure S25).

2.2.2. PXRD (Powder X-ray Diffraction). Powder X-ray diffraction patterns were obtained using an X'Pert X-ray PANalytical diffractometer with an X'accelerator module using Cu $K\alpha$ ($\lambda = 1.5418 \text{ \AA}$) radiation at room temperature, with a step size of 0.02° in two theta (2θ). PXRD patterns of the as-synthesized MOFs confirm that these materials are isostructural to the parent DMOF structure (Figure S2). Moreover, by comparison of as-synthesized samples with the simulated patterns from single crystal X-ray diffraction (Figures S3–S9), phase purity was confirmed. Comparison of PXRD patterns of as-synthesized samples with samples obtained after water exposure and samples obtained after regenerating the water-exposed samples was used to characterize the impact of water adsorption on the crystallinity of the functionalized, isostructural DMOF variations (Figures S10–S12).

2.2.3. N_2 Adsorption Measurements. Nitrogen adsorption measurements (Figures S18–S24) at 77 K were performed for each activated (refer to Table S1 for details on the activation process) MOF before and after water exposure using a Quadasorb system from Quantachrome Instruments. A sample size of approximately 20–30 mg was used to collect these isotherms. Specific surface areas (m^2/g) were determined by applying the BET model to the obtained adsorption isotherms. BET theory was applied over the pressure range $P/P_0 < 0.05$ to ensure that consistent, physically meaningful parameters were obtained.⁴⁶

2.2.4. Thermogravimetric–Mass Spectroscopic (TG-MS) Analysis. Thermogravimetric analyses (TGA) of as-synthesized samples (Figure S14a) of newly synthesized MOFs (DMOF-X, X = MM1, MM2, DM1, and DM2) were carried out under helium in the temperature range 30–600 °C on a NETZSCH STA 449 F1 Jupiter device with a heating rate of 5 °C/min and flow rate of 20 mL/min. To ensure that only half of the BDC ligands are functionalized by the dimethyl functionality in DMOF-DM1, we performed the TG analysis with parallel online mass spectrometric (MS) analysis on the activated DMOF-DM1 sample (Figure S14b).

2.2.5. ^1H Nuclear Magnetic Resonance (H NMR). To confirm the successful synthesis of DMOF-MM1, MM2, and DM1, Varian Mercury Vx 300 was used to record the ^1H NMR spectrum of activated samples of DMOF-MM1, MM2, and DM1 (Figures S15–S17). Small amounts of the activated MOF samples (activated under vacuum at 110 °C for 12 h) were digested with NaOH in D_2O and subsequently subjected to ^1H NMR measurements.

2.2.6. Water Vapor Adsorption Isotherm Measurements. Water vapor adsorption isotherms were measured at 298 K and 1 bar using an IGA-3 (Intelligent Gravimetric Analyzer) series device from Hiden Analytical Ltd. Samples loaded in the IGA-3 device were activated (see Table S1 for details) *in situ* to remove any guest molecules from the structure. A sample size of approximately 30–40 mg was used to collect water adsorption isotherms. Using two mass flow controllers, the ratio of saturated and dry air was varied to control the relative humidity (RH) of the sample environment. Saturated air is generated by bubbling a percentage of dry air through a canister filled with deionized water. For all the experiments, the total gas flow rate was set at 200 cm^3/min . Variable timeouts were used, with a maximum limit of 20 h for each adsorption/desorption point so that sufficient time was available to approach equilibrium for all isotherm points. Because of the possibility of water condensation in the equipment at higher humidities, experiments were conducted only up to 90% RH. After water exposure, samples were regenerated at the activation conditions given in Table S1.

2.3. Computational Methods. All structures used in classical simulations were optimized via periodic quantum mechanics calculations using the VASP package. Ionic relaxations were first performed on the unit cells obtained from experimental CIF files with 400 eV plane wave cutoffs, PAW pseudopotentials,⁴⁷ and the PBE-GGA⁴⁸ until forces on all atoms were less than 30 meV/Å. Tip4P-Ew,⁴⁹ a four-point model optimized for the Ewald charge summation method used in periodic systems, was used to describe water molecules, and framework partial charges were assigned from the quantum-mechanical electrostatic potential via the REPEAT charge-fitting method.⁵⁰ The DREIDING force field⁵¹ was used to obtain Lennard-Jones parameters for all framework atoms, and Lorentz–Berthelot mixing rules were applied to calculate intermolecular van der Waals interactions between water and framework atoms. All transition state calculations were performed using the QST/LST method on Accelrys DMOL3 program at high precision with the DNP basis set, GGA-PBE functional, and all electron treatment of core electrons. Further simulation details can be found in the Supporting Information.

3. RESULTS AND DISCUSSION

3.1. Structure Characterization and Physical Properties. As mentioned before, DMOF-MM1, MM2, DM1, and DM2 are new MOFs. However, we were only able to obtain single crystals for the DMOF-DM1 and DM2 structures. Single crystal X-ray diffraction (XRD) analysis of DMOF-DM1 and DM2 shows that these frameworks are isostructural to the parent DMOF, containing the same $\text{Zn}_2(\text{COO})_4$ paddle-wheel secondary building units (SBUs) bridged by their respective carboxylate BDC ligand to form the 2D layers. DABCO ligands act as pillars by occupying axial sites of the Zn_2 paddle wheels and extending the 2D layers into a 3D structure (Figure S1). Single crystal XRD analysis shows that DMOF-DM1 crystallizes in the $P4/mmm$ space group and, similar to the DMOF-TM1 and TM2 structures reported by Chun et al.,⁴⁵ contains structural disorder in the CIF file. However, DMOF-DM2 crystallizes in $I41/acd$ space group and does not have any disorder. Crystallographic details are listed in the Supporting Information (Table S2 and Figure S25).

To confirm that DMOF-DM1 consists of both BDC and DMBDC, we performed TGA experiments on the activated sample of DMOF-DM1 followed by mass spectrometric (MS) analysis (Figure S14b). Around the decomposition temperature

of DMOF-DM1, we first see the MS signal appear at m/z values of 42 and 55 due to DABCO, followed by CO_2 (at m/z value of 44), benzene (at m/z value of 78), and *p*-xylene (at m/z value of 91, 106). This suggests bond cleavage between the DABCO ligand and the SBU as well as cleavage of the bond of terminal carboxyl groups with both benzene and *p*-xylene rings. Quantitative confirmation that only half of the BDC ligands in DMOF-DM1 contain the dimethyl functionality was obtained using ^1H NMR measurements on the activated DMOF-DM1 sample (Figure S17). Similar logic was given by Chun et al.⁴⁵ to confirm the successful synthesis of DMOF-TM1.

We could not obtain good quality single crystals for DMOF-MM1 and DMOF-MM2, so we again used ^1H NMR to confirm their successful synthesis (Figures S15 and S16). TGA analyses of the as-synthesized samples of DMOFs-MM1, -MM2, -DM1, and -DM2 show that they all decompose in the 250–300 °C range (Figure S14a and Table S1), similar to the parent material.⁵² Comparison of PXRD patterns (Figure S2) of these newly synthesized MOFs with simulated pattern of DMOF also confirm that these MOFs belong to the same isostructural family as DMOF-TM1, DMOF-TM2, and DMOF-TF, which were reported by Chun et al.⁴⁵

The purity of all the synthesized samples can be confirmed by comparing PXRD patterns of as-synthesized MOF samples with patterns simulated from their single crystal structures (Figures S3–S9). Since we could not obtain single crystal structures for DMOF-MM1 and MM2, we used simulated patterns of isostructural MOFs: DMOF-TM1, and TM2. As expected, N_2 adsorption measurements (Figures S18–S24) at 77 K on the activated MOF samples show that a higher degree of functionalization leads to a reduction in porosity (Table 2) compared to the parent MOF. These isotherms showed typical type I behavior according to the IUPAC classification.⁹

Table 2. Comparison of Properties of Isostructural Pillared MOFs

material	pore vol ^a (cm^3/g)	pore diam (<i>c</i> , <i>a</i> , <i>b</i>) (Å)	surface area ^c (m^2/g)		
			before	after ^d	% loss
DMOF ²⁴	0.75	7.5×7.5 , 4.8×3.2 , 4.8×3.2 ^b	1980	7	100
DMOF-MM1	0.76	$<7.5 \times 7.5$, 4.8×3.2 , 4.8×3.2	1856	14	99
DMOF-MM2	0.72	$<7.5 \times 7.5$, 4.8×3.2 , 4.8×3.2	1686	7	100
DMOF-DM1	0.61	5.84×7.5 , –, –	1494	40	97
DMOF-DM2	0.51	5.84 , –, –	1115	14	99
DMOF-TM1 ⁴⁴	0.53	3.5×7.5 , –, – ^b	1210	822	32
DMOF-TM2	0.51	3.5 , –, – ^b	1050	1050	0
DMOF-TF	0.45	6 , –, – ^b	1205	1	100

^aObtained from the Dubinin–Astakov model of N_2 adsorption at 77 K. ^bObtained from the literature.^{24,45} ^cBET analysis.⁴⁶ ^dAfter 90% RH exposure.

3.2. Structural Stability under Humid Conditions.

3.2.1. Water Isotherms, PXRD Patterns, and Surface Areas. Water vapor adsorption isotherm behavior, along with PXRD patterns and BET surface areas before and after water exposure (up to 90% RH), were used to investigate the stability of this isostructural series under humid conditions. The observed trends in water stability indicate that the stability of structures

in this series is directly related to the number and placement of methyl groups on the BDC ligand. The water stability characteristics of these MOFs can be put into three different classifications: fully stable (DMOF-TM2), partially stable (DMOF-TM1), and unstable (all remaining structures). Table 2 shows key structural properties, along with BET surface areas before and after water exposure, for all the different structures. Water isotherms are shown in Figure 2, and

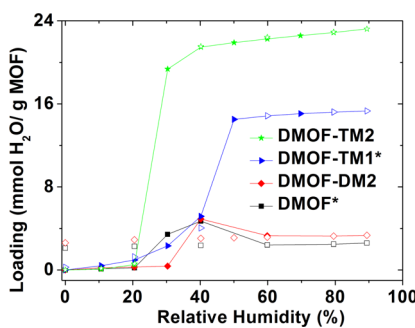


Figure 2. Water vapor adsorption isotherms at 298 K and 1 bar for fully stable (DMOF-TM2), partially stable (DMOF-TM1), and a representative unstable (DMOF-DM2) structure (closed symbols: adsorption; open symbols: desorption). Lines connecting the adsorption points are to guide the eye. Results for the complete collection of MOF materials can be found in the supplemental information. *Reported from our previous work.^{24,44}

PXRD patterns before and after water exposure for the fully stable DMOF-TM2, the partially stable DMOF-TM1, and the unstable DMOF-DM2 structure (representative of all unstable MOFs in this study) are shown in Figure 3. The complete set of PXRD patterns and adsorption isotherms for all the structures in the series can be found in the Supporting Information (Figures S10–S13). In general, adsorption capacities at saturation are dictated by the accessible pore volume. However, this trend breaks down for materials that degrade under the adsorption conditions. Thus, the fully stable DMOF-TM2 undergoes complete pore filling, while the partially stable DMOF-TM1 adsorbs appreciable amounts of water but does not reach the high loadings expected from the pore volume due to the collapse of the structure at high RH. On the other hand, the completely unstable DMOF-DM2 displays adsorption behavior that is very similar to the also unstable parent DMOF.

In our previous study,⁴⁴ DMOF-TM2 showed no loss of surface area or change in crystallinity after prolonged exposure to humid conditions. In the current work, the cyclic stability of this MOF was examined by performing three cycles of water vapor adsorption/desorption measurements on the sample. As shown in Figure 4a, no hysteresis or change in adsorption properties is observed throughout the cyclic adsorption measurements. PXRD patterns (Figure 4b) and BET surface area show no change in the crystal structure even after three adsorption/desorption cycles. DMOF-TM2 was also found to maintain its crystallinity after exposure to lab air for approximately one year (Figure 4c). Given the complete loss of crystallinity and surface area for the parent DMOF structure,²⁴ the stability of this functionalized variation after high water uptake is remarkable; only a few structures, such as UiO-66 and members of the MIL series of materials, are reported to exhibit such stability after adsorbing large amounts of water.^{24,30,32,33} MOF-74 materials were also shown to be completely stable during cyclic dehydration/rehydration experi-

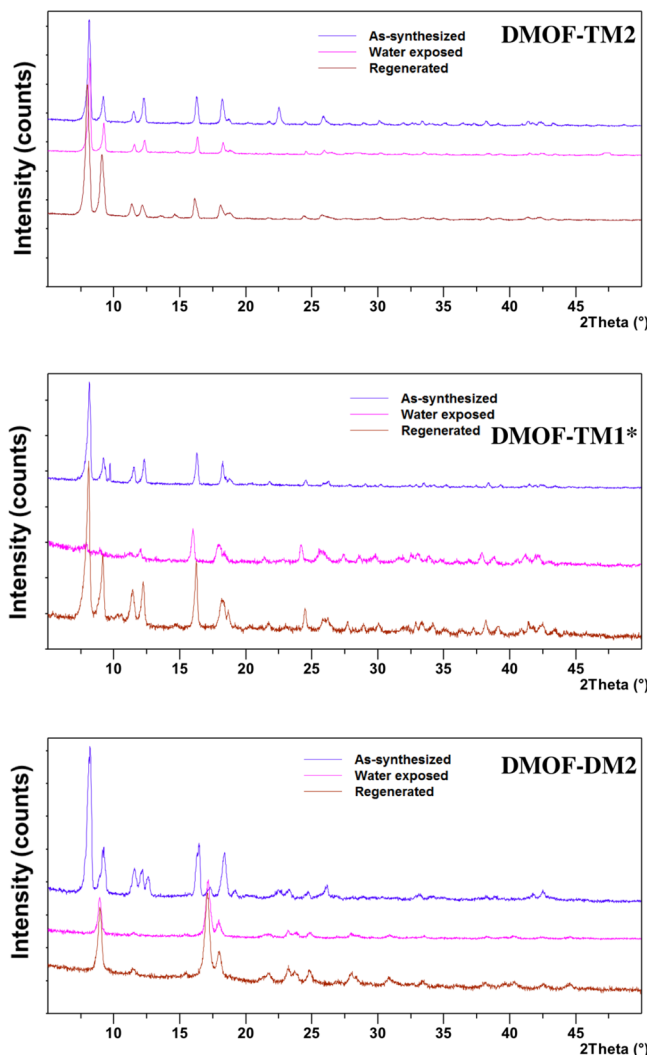


Figure 3. Change in PXRD patterns before and after water exposure (up to 90% RH) for fully stable (DMOF-TM2, top), partially stable (DMOF-TM1, middle), and a representative unstable (DMOF-DM2, bottom) structure. Results for the complete collection of MOF materials can be found in the Supporting Information. *Reported from our previous work.⁴⁴

ments by Dietzel and co-workers. However, it was possible only under inert environment (Ar/N₂).^{53,54} For example, Ni-MOF-74 was reported to decompose in the presence of air during identical testing.⁵⁵ Similarly, Schoenecker et al.²⁴ also found that Mg-MOF-74 decomposes upon exposure to air with 90% RH in the first adsorption/desorption cycle.

Interestingly, the DMOF-TM1 structure, containing equal amounts of the tetramethyl and unfunctionalized variations of BDC, was the only partially stable MOF identified in this series. For this structure, the same type V adsorption behavior found in DMOF-TM2 was observed during the vapor adsorption isotherm; however, the loss of BET surface area (~30%) and crystallinity (Figure 3) after water adsorption measurements indicates that the structure does not have the same structural stability as the DMOF-TM2 variation under humid conditions. Furthermore, despite the greater pore volume of the DMOF-TM1 structure, it has a lower saturation uptake than the DMOF-TM2 structure as well. These findings highlight the importance of the tetramethyl BDC ligand in providing stability in these structures. While a 50:50 ratio of the tetramethyl BDC

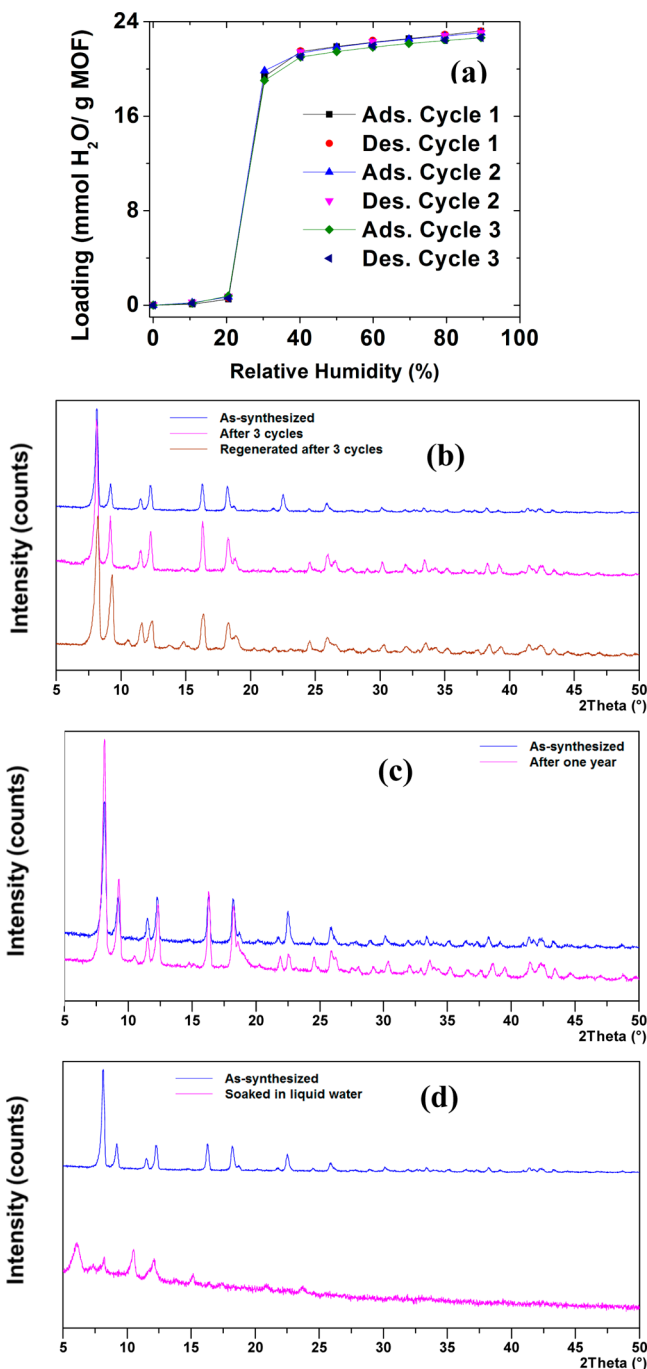


Figure 4. (a) Cyclic water vapor adsorption isotherms at 298 K and 1 bar for DMOF-TM2. Lines connecting the adsorption points are to guide the eye. (b) PXRD patterns before and after cyclic water vapor adsorption measurements (up to 90% RH) for DMOF-TM2. (c) PXRD pattern after aging of DMOF-TM2 under ambient conditions for one year. (d) Change in PXRD pattern upon soaking DMOF-TM2 in liquid water for 24 h.

and BDC ligands is enough to create a partially stable MOF, only through full ligand incorporation of the tetramethyl can complete stability be achieved. In contrast, the DMOF-DM2 structure contains the same relative number of methyl groups per unit cell as DMOF-TM1 yet, as discussed in the following section, is found to be completely unstable in the presence of water (Figures 2 and 3). This further suggests that the number of nonpolar groups alone is not enough to dictate water

stability; instead, the precise placement of methyl groups on the BDC ligand is critically important to the water stability. Ma et al.¹⁵ also observed a similar trend; however, in their publication the pillar ligand (BPy) was modified rather than the carboxylate ligand (BDC).

All of the remaining structures were found to be fully unstable after 90% RH exposure. These structures, containing varying amounts of nonpolar (MM1, MM2, DM1, DM2) and polar (fluorine) functional groups on the BDC ligand, exhibited significant structural decay in the presence of humid conditions. This is indicated by both the shape of their adsorption isotherms (leveling off well below their expected saturation uptakes values) and the complete loss of crystallinity and surface area observed during their subsequent characterization after water adsorption. Furthermore, the residual water content present in these structures after complete desorption to 0% RH conditions suggests that all the water adsorbed in the structures is not physisorbed and, instead, some fraction participates in irreversible hydrolysis reactions with the zinc metal in the structure. Notably, it was found that DMOF-TF, a functionalized structure with full incorporation of polar, fluorine groups through the tetrafluoro-BDC ligand, also did not result in the same improvement in water stability as the DMOF-TM2 variation. This suggests that greater shielding due to the larger van der Waals radii of fluorine and methyl groups (1.5 and 2.0 Å) versus that of hydrogen (1.3 Å) is not the only factor contributing to water stability, and factors such as the polarity of the functional groups must also be considered. In previous work,⁴⁴ we showed the same water instability is present for other members of the isostructural DMOF family containing larger, polar functional groups such as $-NO_2$ and $-OH$, but these groups were present on a single aromatic carbon while the fluoro groups functionalize all four sites in this work. Molecular insight into why this is the case is further explored in the Computational Results section.

3.2.2. Kinetic versus Thermodynamic Stability. In order to understand the water stability trends in this series of MOFs, it is important first to discern whether thermodynamic or kinetic stability trends are what govern the behavior of these structures. While a MOF that is thermodynamically stable in the presence of water is such because the change in free energy (ΔG°) of a hydrolysis reaction is not favored, in kinetically stable MOFs, the stability instead relies on there being a sufficiently high activation energy barrier (E_a) for the hydrolysis reaction. As mentioned earlier, the strength of Lewis acid–base interactions can be used to rationalize thermodynamic stability trends, whereas other more complex structural considerations are needed to understand the activation energy barrier for kinetically governed ligand displacement reactions to occur.

To ensure we are investigating the correct phenomena in our series of MOFs, experiments were performed on these structures to confirm the observed breakdown mechanisms were purely kinetic in nature. The first evidence of the purely kinetic stability in these MOFs came from immersing the DMOF-TM2 structure in liquid water at room temperature for 24 h. Subsequent structural analysis after liquid water exposure indicated a complete loss of crystallinity (Figure 4d). Second, the trends in water stability observed in the different MOF structures were compared to the predicted thermodynamic stability based on the pK_a of the different BDC ligands (Table 3). If the trends were thermodynamic in nature, one would expect the stability trends to correlate directly with ligand pK_a ; on the contrary, the cyclically stable DMOF-TM2 (TMBDC,

Table 3. Comparison of pK_a Values³⁷ of Functionalized BDC Ligands in Isostructural Pillared MOFs (DMOF-X)

MOF	carboxylate ligand	pK_a
DMOF	BDC	3.73
DMOF-MM2	MMBDC	3.76 ^a
DMOF-DM2	DMBDC	3.77
DMOF-TM2	TMBDC	3.80
DMOF-MM1	BDC, MMBDC	3.73, 3.76 ^a
DMOF-DM1	BDC, DMBDC	3.73, 3.77
DMOF-TM1	BDC, TMBDC	3.73, 3.80
DMOF-TF	TFBDC	1.42

^aAverage of two pK_a values arising due to asymmetry of monofunctionalization.

$pK_a = 3.80$) and partially stable DMOF-TM1 (TMBDC, $pK_a = 3.80$ and BDC, $pK_a = 3.73$) structures contain ligands with pK_a values that are very similar to the remaining unstable MOFs grafted with nonpolar groups ($pK_a = 3.73\text{--}3.77$), indicating that there is no correlation between expected thermodynamic stability trends and our observed trends in water stability.

3.2.3. Computational Results. In order for a ligand displacement hydrolysis reaction to occur between the nucleophilic oxygen on a water molecule (denoted O_w) and an electrophilic zinc (Zn), two molecular events must occur. First, the adsorbed water molecules must come close enough to the Zn metal to allow significant interaction to occur between the Zn and O_w electron orbitals, and second, the energetics of this interaction must be such that the kinetic barrier to a ligand substitution reaction can be overcome. The first event, dealing with the proximity of O_w and Zn within a structure, can be addressed through classical molecular dynamics simulations, whereas the second question, dealing with the kinetic barriers to reaction, can only be addressed through a more detailed quantum-mechanical description of the system.

To investigate the first question, classical Monte Carlo simulations with the Tip4p-Ew water model were run in the DMOF, DMOF-TF, and DMOF-TM2 structures. These structures were chosen for the simulations as they represent both stable (DMOF-TM2) and unstable (DMOF, DMOF-TF) structures with no shielding (DMOF), shielding via polar groups (DMOF-TF), and shielding via nonpolar groups (DMOF-TM2). Simulations were run under the approximate loadings present in the DMOF at the onset of structural breakdown, as indicated by the change in shape of the DMOF adsorption isotherm (occurring at ~ 4.6 mol/kg water loading). The accurate prediction of bond breakage and formation using classical simulations is especially difficult, given the generic nature of classical force fields. Thus, the goal of these simulations was not to capture ligand substitution events occurring in the system, but instead to provide insight into any differences in water behavior present in the DMOF-TM2 vs DMOF and DMOF-TF structures that make the former structure stable and the latter structures unstable. An investigation into the partial stability of the DMOF-TM1 structure would also be of interest, but given the large disorder present in the experimental CIF file for this structure, it is impossible to assign locations to the 50% TMBDC and 50% BDC ligands present in the structure.

Figure 5 shows the water density distributions obtained from these simulations. The pronounced difference in water confinement within the pores, evident from the density distributions shown in the *c*-direction, provides important

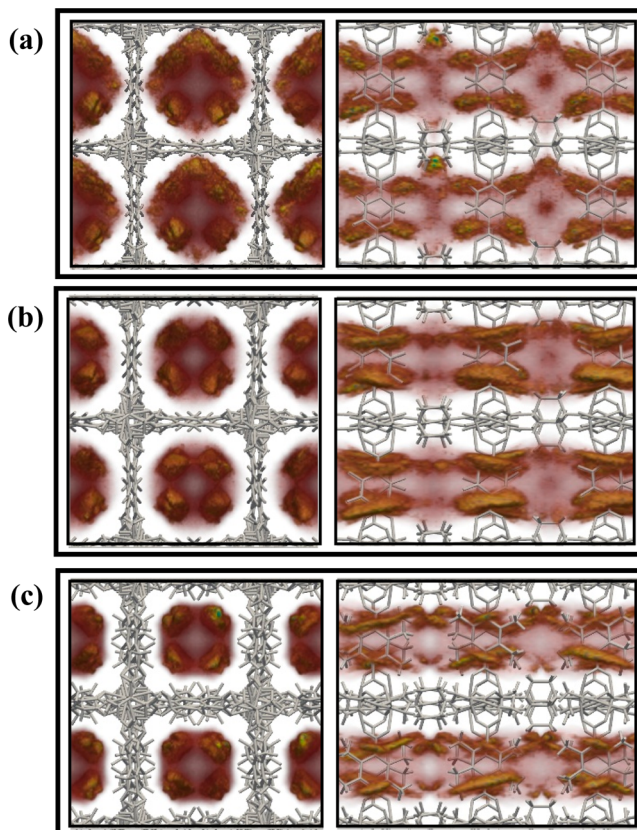


Figure 5. Water density distributions for DMOF (a), DMOF-TF (b), and DMOF-TM2 (c) structures shown in the *c*-direction (left) and *a*-direction (right).

insight into the observed differences in kinetic water stability within these systems. While the frameworks were treated as rigid in these simulations, the parent DMOF is known to be weakly flexible and, in the presence of adsorbates such as benzene and isopropyl alcohol,^{43,56} reported to exhibit breathing behavior. In the case of isopropyl alcohol, hydrogen-bonding interactions between the OH group on the adsorbate and the oxygen atoms on the BDC ligand were shown to induce a structural transformation from the native wide pore conformation to a narrow pore conformation in the framework.⁵⁷ As a result, it is expected that the water molecules near the BDC ligand present in the DMOF and, to a lesser degree, DMOF-TF structures would cause the same structural transformation to occur. The result of this breathing behavior, depicted in Figure 6, is the likely explanation for the poor structural stability in DMOF and DMOF-TF (along with the other unstable MOFs observed in this study). After this structural change occurs, water is able to come much closer to the zinc hydrolysis sites located at the pore corners with greater than 90° angles. It is important to note that, while this same breathing behavior was observed in the parent DMOF structure during isopropyl adsorption, no alcoholysis reaction was observed because of the weaker nucleophilicity of this adsorbate relative to water (due to steric effects). In the case of DMOF-TM2, the structure is fully stable because no water molecules are able to come close enough to the BDC ligand to participate in hydrogen-bonding interactions (due to shielding effects from the nonpolar methyl groups).

In order to investigate the second prerequisite to a ligand displacement reaction, dealing with the activation energy

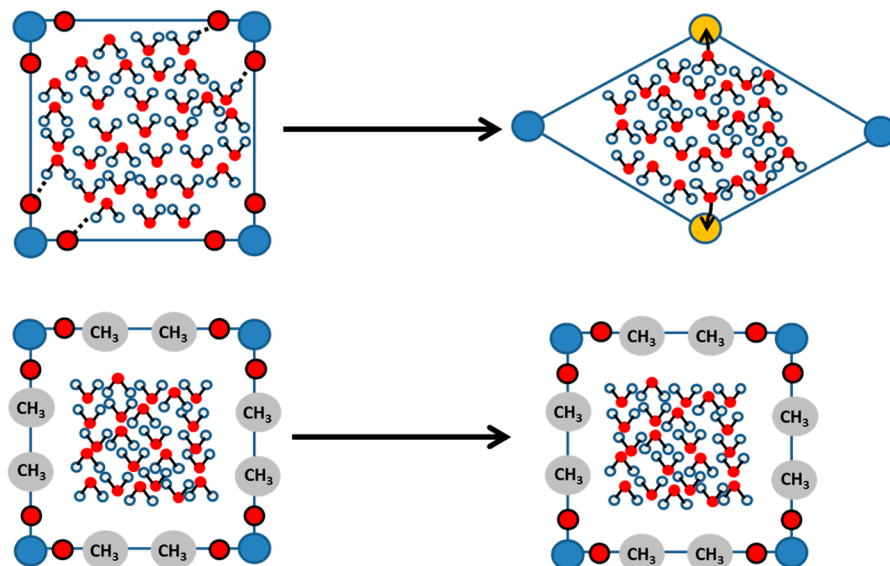


Figure 6. Schematic of likely structural transformations, shown in the *c*-direction, for DMOF and DMOF-TM2 structures in the presence of water. The large red circles depict carboxylate oxygens, small red and white circles portray oxygen and hydrogen atoms in water, respectively, and large blue circles represent stable Zn clusters. The large yellow circles denote Zn clusters that will be prone to hydrolysis.

barrier to reaction once water is sufficiently close to a zinc atom, quantum-mechanical calculations were performed on chemical clusters that are representative of the DMOF and DMOF-TM2 structures. This technique, similar to the approach used by Low et al.,¹⁹ assumes that the behavior of a truncated MOF cluster is representative of the behavior observed in the true periodic system. Figure 7 shows the

reactants and products of two possible ligand displacement mechanisms involving the interaction of a single water molecule with zinc to displace either the BDC or DABCO ligand. Interestingly, these calculations failed to qualitatively capture the experimentally observed trends in kinetic water stability in the system. While the barrier to a displacement reaction involving DABCO was found to be much higher (~2–3 times) than the barrier associated with BDC, the trends in activation energy for the BDC ligand in DMOF (15.8 kcal/mol) versus DMOF-TM2 (9.1 kcal/mol) followed trends that were opposite of what was expected from experiment. The deficiencies of a clustering approach in finding appropriate activation energies in MOF systems are noteworthy and suggest that more detailed, periodic treatments of such systems are necessary in order determine accurate kinetics information in MOFs. The likely reason for these discrepancies arises from the unphysical dynamics that are introduced when treating crystalline structures as nonperiodic clusters; without the structural constraints arising from the interconnected metal clusters in truly periodic systems, clusters are able to achieve bending and torsion angles during hydrolysis reactions that would be highly unphysical in the real system. Furthermore, the sterics of the adjacent methyl groups present in the periodic DMOF-TM2 system would also create large energetic penalties to a ligand displacement reaction that are not captured in the consideration of only one isolated cluster.

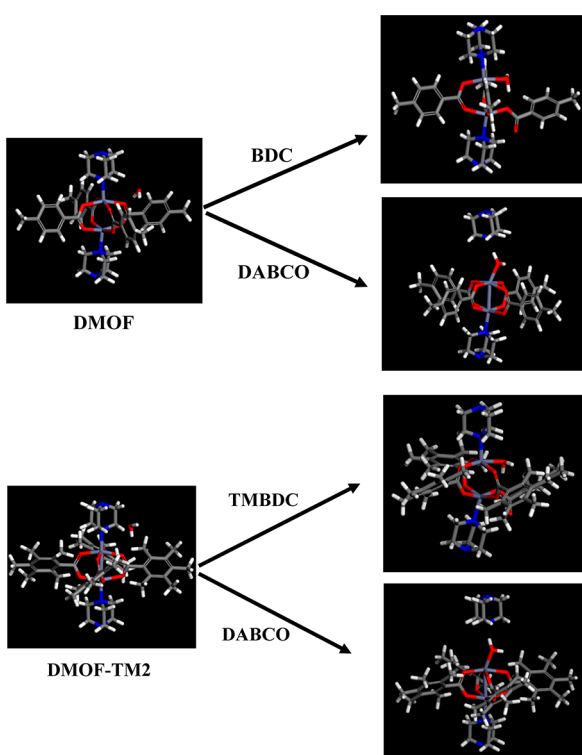


Figure 7. Product and reactant clusters used in quantum-mechanical calculations for determining barriers to the ligand displacement reactions involving BDC and DABCO in the DMOF and DMOF-TM2 structures.

4. CONCLUSIONS

In this work, we have carried out a systematic study into the effects of ligand functionalization on the water stability of a series of isostructural MOFs of the family $Zn(BDC-X)-(DABCO)_{0.5}$. We shed light on the important distinction between kinetic and thermodynamic water stability and provide experimental evidence for a kinetically governed water stability mechanism in these MOFs. In this case, the full incorporation of nonpolar methyl groups is critical to promoting the cyclic stability in this series. As such, we show that the kinetically unstable parent structure can be made cyclically stable in the presence of humid conditions through the incorporation

tetramethyl-BDC ligand. Given the large water uptake in this methyl functionalized structure, we show that the water stability improvement in this MOF is not due to the exclusion of water from entering the pores of the MOF. Through molecular simulations we show that the reason for the improvement in kinetic stability is due to shielding of the carboxylate oxygen in the DMOF-TM2 structure which prevents hydrogen-bonding interactions and subsequent structural transformations from occurring. As a result, the electrophilic zinc atoms in this structure are inaccessible to the nucleophilic oxygen atoms in water, thus preventing any ligand displacement hydrolysis reactions from occurring. This systematic study provides initial insight into important structural factors that are important for the development of next-generation, water-stable metal-organic frameworks.

■ ASSOCIATED CONTENT

Supporting Information

Further computational details, synthesis procedures, PXRD patterns, and water vapor and N₂ adsorption isotherms. This material is available free of charge via the Internet at <http://pubs.acs.org>.

■ AUTHOR INFORMATION

Corresponding Author

*E-mail krista.walton@chbe.gatech.edu; Fax +1-404-894-2866; Tel +1-404-894-5254.

Notes

The authors declare no competing financial interest.

■ ACKNOWLEDGMENTS

This material is based upon work supported by Army Research Office PECASE Award W911NF-10-1-0079 and Contract W911NF-10-1-0076. Computational resources were also provided by the Extreme Science and Engineering Discovery Environment (XSEDE), which is supported by the National Science Foundation Grant OCI-1053575. The authors would also like to thank Dr. David Dubbeldam for invaluable discussions on performing the computational study.

■ REFERENCES

- (1) Zhou, H. C.; Long, J. R.; Yaghi, O. M. Introduction to metal-organic frameworks. *Chem. Rev.* **2012**, *112* (2), 673–674.
- (2) Rowsell, J. L. C.; Yaghi, O. M. Effects of functionalization, catenation, and variation of the metal oxide and organic linking units on the low-pressure hydrogen adsorption properties of metal-organic frameworks. *J. Am. Chem. Soc.* **2006**, *128* (4), 1304–1315.
- (3) Cook, T. R.; Zheng, Y.-R.; Stang, P. J. Metal-organic frameworks and self-assembled supramolecular coordination complexes: comparing and contrasting the design, synthesis, and functionality of metal-organic materials. *Chem. Rev.* **2012**, DOI: 10.1021/cr3002824.
- (4) Farha, O. K.; Hupp, J. T. Rational design, synthesis, purification, and activation of metal-organic framework materials. *Acc. Chem. Res.* **2010**, *43* (8), 1166–1175.
- (5) Tanabe, K. K.; Cohen, S. M. Postsynthetic modification of metal-organic frameworks—a progress report. *Chem. Soc. Rev.* **2011**, *40* (2), 498–519.
- (6) Eddaoudi, M.; Kim, J.; Rosi, N.; Vodak, D.; Wachter, J.; O’Keeffe, M.; Yaghi, O. M. Systematic design of pore size and functionality in isoreticular MOFs and their application in methane storage. *Science* **2002**, *295* (5554), 469–472.
- (7) Ferey, G. Some suggested perspectives for multifunctional hybrid porous solids. *Dalton Trans.* **2009**, *23*, 4400–4415.
- (8) Kuppler, R. J.; Timmons, D. J.; Fang, Q. R.; Li, J. R.; Makal, T. A.; Young, M. D.; Yuan, D. Q.; Zhao, D.; Zhuang, W. J.; Zhou, H. C. Potential applications of metal-organic frameworks. *Coord. Chem. Rev.* **2009**, *259* (23–24), 3042–3066.
- (9) Kitagawa, S.; Kitaura, R.; Noro, S. Functional porous coordination polymers. *Angew. Chem., Int. Ed.* **2004**, *43* (18), 2334–2375.
- (10) Sumida, K.; Rogow, D. L.; Mason, J. A.; McDonald, T. M.; Bloch, E. D.; Herm, Z. R.; Bae, T.-H.; Long, J. R. Carbon dioxide capture in metal-organic frameworks. *Chem. Rev.* **2011**, *112* (2), 724–781.
- (11) Li, J.-R.; Kuppler, R. J.; Zhou, H.-C. Selective gas adsorption and separation in metal-organic frameworks. *Chem. Soc. Rev.* **2009**, *38* (5), 1477–1504.
- (12) Karra, J. R.; Walton, K. S. Effect of open metal sites on adsorption of polar and nonpolar molecules in metal-organic framework Cu-BTC. *Langmuir* **2008**, *24* (16), 8620–8626.
- (13) Mueller, U.; Schubert, M.; Teich, F.; Puetter, H.; Schierle-Arndt, K.; Pastre, J. Metal-organic frameworks - prospective industrial applications. *J. Mater. Chem.* **2006**, *16* (7), 626–636.
- (14) Li, Y.; Yang, R. T. Gas adsorption and storage in metal-organic framework MOF-177. *Langmuir* **2007**, *23* (26), 12937–12944.
- (15) Ma, D.; Li, Y.; Li, Z. Tuning the moisture stability of metal-organic frameworks by incorporating hydrophobic functional groups at different positions of ligands. *Chem. Commun.* **2011**, *47* (26), 7377–7379.
- (16) Yang, J.; Grzech, A.; Mulder, F. M.; Dingemans, T. J. Methyl modified MOF-5: a water stable hydrogen storage material. *Chem. Commun.* **2011**, *47* (18), 5244–5246.
- (17) Choi, H. J.; Dinca, M.; Dailly, A.; Long, J. R. Hydrogen storage in water-stable metal-organic frameworks incorporating 1,3-and 1,4-benzenedipyrizolate. *Energy Environ. Sci.* **2010**, *3* (1), 117–123.
- (18) Kaye, S. S.; Dailly, A.; Yaghi, O. M.; Long, J. R. Impact of preparation and handling on the hydrogen storage properties of Zn₄O(1,4-benzenedicarboxylate)₃ (MOF-5). *J. Am. Chem. Soc.* **2007**, *129* (46), 14176–+.
- (19) Low, J. J.; Benin, A. I.; Jakubczak, P.; Abrahamian, J. F.; Faheem, S. A.; Willis, R. R. Virtual high throughput screening confirmed experimentally: porous coordination polymer hydration. *J. Am. Chem. Soc.* **2009**, *131* (43), 15834–15842.
- (20) Kang, I. J.; Khan, N. A.; Haque, E.; Jhung, S. H. Chemical and thermal stability of isotopic metal-organic frameworks: effect of metal ions. *Chem.—Eur. J.* **2011**, *17* (23), 6437–6442.
- (21) Kim, M.; Cohen, S. M. Discovery, development, and functionalization of Zr(IV)-based metal-organic frameworks. *CrystEngComm* **2012**, *14* (12), 4096–4104.
- (22) Cavka, J. H.; Jakobsen, S.; Olsbye, U.; Guillou, N.; Lamberti, C.; Bordiga, S.; Lillerud, K. P. A new zirconium inorganic building brick forming metal organic frameworks with exceptional stability. *J. Am. Chem. Soc.* **2008**, *130* (42), 13850–13851.
- (23) Garibay, S. J.; Cohen, S. M. Isoreticular synthesis and modification of frameworks with the UiO-66 topology. *Chem. Commun.* **2010**, *46* (41), 7700–7702.
- (24) Schoenecker, P. M.; Carson, C. G.; Jasuja, H.; Flemming, C. J. J.; Walton, K. S. Effect of water adsorption on retention of structure and surface area of metal-organic frameworks. *Ind. Eng. Chem. Res.* **2012**, *51* (18), 6513–6519.
- (25) Cychosz, K. A.; Matzger, A. J. Water stability of microporous coordination polymers and the adsorption of pharmaceuticals from water. *Langmuir* **2010**, *26* (22), 17198–17202.
- (26) Greathouse, J. A.; Allendorf, M. D. The interaction of water with MOF-5 simulated by molecular dynamics. *J. Am. Chem. Soc.* **2006**, *128* (33), 10678–10679.
- (27) Bellarosa, L.; Calero, S.; Lopez, N. Early stages in the degradation of metal-organic frameworks in liquid water from first-principles molecular dynamics. *Phys. Chem. Chem. Phys.* **2012**, *14* (20), 7240–7245.
- (28) Han, S. S.; Choi, S. H.; van Duin, A. C. T. Molecular dynamics simulations of stability of metal-organic frameworks against H₂O using

- the ReaxFF reactive force field. *Chem. Commun.* **2010**, *46* (31), 5713–5715.
- (29) Colombo, V.; Galli, S.; Choi, H. J.; Han, G. D.; Maspero, A.; Palmisano, G.; Masciocchi, N.; Long, J. R. High thermal and chemical stability in pyrazolate-bridged metal-organic frameworks with exposed metal sites. *Chem. Sci.* **2011**, *2* (7), 1311–1319.
- (30) Kuesgens, P.; Rose, M.; Senkovska, I.; Froede, H.; Henschel, A.; Siegle, S.; Kaskel, S. Characterization of metal-organic frameworks by water adsorption. *Microporous Mesoporous Mater.* **2009**, *120* (3), 325–330.
- (31) Liang, Z.; Marshall, M.; Chaffee, A. L. CO₂ adsorption, selectivity and water tolerance of pillared-layer metal organic frameworks. *Microporous Mesoporous Mater.* **2010**, *132* (3), 305–310.
- (32) Soubeyrand-Lenoir, E.; Vagner, C.; Yoon, J. W.; Bazin, P.; Ragon, F.; Hwang, Y. K.; Serre, C.; Chang, J.-S.; Llewellyn, P. L. How water fosters a remarkable 5-fold increase in low-pressure CO₂ uptake within mesoporous MIL-100(Fe). *J. Am. Chem. Soc.* **2012**, *134* (24), 10174–10181.
- (33) Wiersum, A. D.; Soubeyrand-Lenoir, E.; Yang, Q. Y.; Moulin, B.; Guillerm, V.; Ben Yahia, M.; Bourrelly, S.; Vimont, A.; Miller, S.; Vagner, C.; Daturi, M.; Clet, G.; Serre, C.; Maurin, G.; Llewellyn, P. L. An evaluation of UiO-66 for gas-based applications. *Chem.—Asian J.* **2011**, *6* (12), 3270–3280.
- (34) Valenzano, L.; Civalleri, B.; Chavan, S.; Bordiga, S.; Nilsen, M. H.; Jakobsen, S.; Lillerud, K. P.; Lamberti, C. Disclosing the complex structure of UiO-66 metal organic framework: a synergic combination of experiment and theory. *Chem. Mater.* **2011**, *23* (7), 1700–1718.
- (35) Liang, Z.; Marshall, M.; Chaffee, A. L. CO₂ adsorption-based separation by metal organic framework (Cu-BTC) versus zeolite (13X). *Energy Fuels* **2009**, *23*, 2785–2789.
- (36) Mohamed, M. H.; Elsaidi, S. K.; Wojtas, L.; Pham, T.; Forrest, K. A.; Tudor, B.; Space, B.; Zaworotko, M. J. Highly selective CO₂ uptake in uninodal 6-connected “mmo” nets based upon MO₄²⁻ (M = Cr, Mo) pillars. *J. Am. Chem. Soc.* **2012**, DOI: 10.1021/ja309452y.
- (37) Hilal, S.; Karickhoff, S. W.; Carreira, L. A. A rigorous test for SPARC’s chemical reactivity models: estimation of more than 4300 ionization pKa’s. *Quant. Struct.-Act. Relat.* **1995**, *14*, 348.
- (38) Wu, T.; Shen, L.; Luebbers, M.; Hu, C.; Chen, Q.; Ni, Z.; Masel, R. I. Enhancing the stability of metal-organic frameworks in humid air by incorporating water repellent functional groups. *Chem. Commun.* **2010**, *46*, 33.
- (39) Nguyen, J. G.; Cohen, S. M. Moisture-resistant and superhydrophobic metal-organic frameworks obtained via postsynthetic modification. *J. Am. Chem. Soc.* **2010**, *132* (13), 4560.
- (40) Cai, Y.; Zhang, Y. D.; Huang, Y. G.; Marder, S. R.; Walton, K. S. Impact of alkyl-functionalized btc on properties of copper-based metal-organic frameworks. *Crys. Growth Des.* **2012**, *12* (7), 3709–3713.
- (41) Serre, C. Superhydrophobicity in highly fluorinated porous metal-organic frameworks. *Angew. Chem., Int. Ed.* **2012**, *51* (25), 6048–6050.
- (42) Taylor, J. M.; Vaidhyanathan, R.; Iremonger, S. S.; Shimizu, G. K. H. Enhancing Water Stability of Metal–Organic Frameworks via Phosphonate Monoester Linkers. *J. Am. Chem. Soc.* **2012**, *134* (35), 14338–14340.
- (43) Dybtsev, D. N.; Chun, H.; Kim, K. Rigid and flexible: A highly porous metal-organic framework with unusual guest-dependent dynamic behavior. *Angew. Chem., Int. Ed.* **2004**, *43* (38), 5033–5036.
- (44) Jasuja, H.; Huang, Y.; Walton, K. S. Adjusting the stability of metal-organic frameworks under humid conditions by ligand functionalization. *Langmuir* **2012**, *28*, 16874–16880.
- (45) Chun, H.; Dybtsev, D. N.; Kim, H.; Kim, K. Synthesis, X-ray crystal structures, and gas sorption properties of pillared square grid nets based on paddle-wheel motifs: implications for hydrogen storage in porous materials. *Chem.—Eur. J.* **2005**, *11* (12), 3521–3529.
- (46) Walton, K. S.; Snurr, R. Q. Applicability of the BET method for determining surface areas of microporous metal-organic frameworks. *J. Am. Chem. Soc.* **2007**, *129* (27), 8552–8556.
- (47) Blochl, P. E. Projector augmented-wave method. *Phys. Rev. B* **1994**, *50* (24), 17953–17979.
- (48) Perdew, J. P.; Burke, K.; Ernzerhof, M. Generalized gradient approximation made simple. *Phys. Rev. Lett.* **1996**, *77* (18), 3865–3868.
- (49) Horn, H. W.; Swope, W. C.; Pitera, J. W.; Madura, J. D.; Dick, T. J.; Hura, G. L.; Head-Gordon, T. Development of an improved four-site water model for biomolecular simulations: TIP4P-Ew. *J. Chem. Phys.* **2004**, *120* (20), 9665–9678.
- (50) Campana, C.; Mussard, B.; Woo, T. K. Electrostatic potential derived atomic charges for periodic systems using a modified error functional. *J. Chem. Theory Comput.* **2009**, *5* (10), 2866–2878.
- (51) Mayo, S. L.; Olafson, B. D.; Goddard, W. A. DREIDING - a generic force-field for molecular simulations. *J. Phys. Chem.* **1990**, *94* (26), 8897–8909.
- (52) Lee, J. Y.; Olson, D. H.; Pan, L.; Emge, T. J.; Li, J. Microporous metal–organic frameworks with high gas sorption and separation capacity. *Adv. Funct. Mater.* **2007**, *17* (8), 1255–1262.
- (53) Dietzel, P. D. C.; Morita, Y.; Blom, R.; Fjellvag, H. An in situ high-temperature single-crystal investigation of a dehydrated metal-organic framework compound and field-induced magnetization of one-dimensional metallocxygen chains. *Angew. Chem., Int. Ed.* **2005**, *44* (39), 6354–6358.
- (54) Dietzel, P. D. C.; Blom, R.; Fjellvag, H. Base-induced formation of two magnesium metal-organic framework compounds with a bifunctional tetratopic ligand. *Eur. J. Inorg. Chem.* **2008**, *23*, 3624–3632.
- (55) Dietzel, P. D. C.; Panella, B.; Hirscher, M.; Blom, R.; Fjellvag, H. Hydrogen adsorption in a nickel based coordination polymer with open metal sites in the cylindrical cavities of the desolvated framework. *Chem. Commun.* **2006**, *9*, 959–961.
- (56) Uemura, K.; Yamasaki, Y.; Komagawa, Y.; Tanaka, K.; Kita, H. Two-step adsorption/desorption on a jungle-gym-type porous coordination polymer. *Angew. Chem., Int. Ed.* **2007**, *46* (35), 6662–6665.
- (57) Grosch, J. S.; Paesani, F. Molecular-level characterization of the breathing behavior of the jungle-gym-type DMOF-1 metal-organic framework. *J. Am. Chem. Soc.* **2012**, *134* (9), 4207–4215.